Molecular Cancer

RESEARCH

Open Access

The EGR1-mediated lncRNA TENM3-AS1 potentiates gastric cancer metastasis via reprogramming fatty acid metabolism

Yuhui Tang[1†], Baiwei Zhao[1†], Wanchuan Wang[2†], Haoming Chen[3], Junsheng Zhang[1], Yi Xie[1], Yongming Chen[1], Feizhi Lin[1], Yuanfang Li[1*], Xiaohui Zhai[4*] and Wen Zhou[2*]

Abstract

Background Long non-coding RNAs (lncRNAs) are essential modulators in tumor progression. While fatty acid (FA) metabolism can potentiate tumorigenesis, colonization, and metastasis, the roles of lncRNAs in reprograming FA metabolism and regulating gastric cancer (GC) metastasis remain elusive.

Methods Whole RNA-sequencing and in silico analyses were conducted to identify clinically significant lncRNAs involved in GC metastasis. Among the identified lncRNAs, we focused on the novel lncRNA TENM3-AS1. RT-qPCR and FISH analyses revealed an increased expression of TENM3-AS1 in GC cell lines and patients. In vitro and in vivo functional experiments validated the effects of TENM3-AS1 to GC metastasis and the reprogramming of FA metabolism. ChIP, Biotinylated RNA pull-down, RIP, CHX-chase assay, ubiquitination assay, and RNA stabilization assay were employed to perceive the mechanisms underlying the effects of TENM3-AS1 in GC cells.

Results TENM3-AS1 expression was significantly elevated in metastatic tumors and advanced primary tumors of GC patients. This increased expression was also associated with a worsened overall survival and progression-free survival. Functionally, TENM3-AS1 enhanced the migration and invasiveness of GC cells in vitro, promoted tumorigenesis and liver metastasis in vivo, and increased FA biosynthesis in GC cells. Mechanistically, our studies showed that the transcription factor EGR1 activated TENM3-AS1, which in turn upregulated the expression of FASN and hnRNPK. Furthermore, TENM3-AS1 interacted with and stabilized hnRNPK by increasing its deubiquitination. This interaction reprogrammed FA metabolism and promoted GC progression by increasing FASN mRNA stability through hnRNPK.

Conclusions In this study, by comparing lncRNA sequencing data from paired primary and peritoneal metastatic tumors and public transcriptome data from non-metastatic and metastatic samples, we clarified a novel lncRNA,

†Yuhui Tang, Baiwei Zhao and Wanchuan Wang contributed equally to this work and shared first authorship.

*Correspondence:
Yuanfang Li
liyuanf@sysucc.org.cn
Xiaohui Zhai
zhaixh@mail.sysu.edu.cn
Wen Zhou
lyzhouw@scut.edu.cn

Full list of author information is available at the end of the article

TENM3-AS1. It was found that TENM3-AS1 was aberrantly activated in metastatic and advanced primary tumors, and was strongly correlated with a shorter survival in GC patients. Our study reveals the EGR1/TENM3-AS1/ hnRNPK/FASN axis as a novel curative target in metastatic GC.

Keywords TENM3-AS1, HNRNPK, FASN, Gastric cancer metastasis, Fatty acid metabolism

Introduction

Gastric cancer (GC) ranks as the fifth leading cause of cancer-related morbidity and mortality worldwide in 2022, due to its aggressive nature and the frequent diagnosis at advanced stages [1, 2]. In spite of advancements in systemic chemotherapy, targeted therapy, and immunotherapy, metastasis often spread to the liver and peritoneum threatening the survival of GC patients [3, 4]. Notably, treating GC patients with peritoneal metastasis is challenging owing to the limited penetration of current chemotherapeutic drugs into the peritoneal cavity [5]. Therefore, identifying novel biomarkers and developing advanced targeted therapies are essential for early diagnosis and appropriate treatment of GC patients with metastasis.

Accumulating evidence suggests that deregulated cellular metabolism supports nutrient acquisition, rapid proliferation, metastatic colonization, and activation of carcinogenic signaling pathways in tumor cells [6–8]. Among various forms of metabolic reprogramming, fatty acid (FA) metabolism, which primarily involves the biosynthesis, transport, catabolism, and oxidation of fatty acids, has gained increasing interest because of its essential role in tumorigenesis, cancer metastasis, and drug resistance [9, 10]. For example, aberrant activation of fatty acid synthase (FASN) has been linked to the increased stemness and a poorer prognosis in HER2 + GC patients [11]. In addition, FA translocase CD36 facilitates GC metastasis by activating AKT/GSK-3β/β-catenin signaling pathway [12]. Nonetheless, the complexity of underlying mechanisms by which FA metabolism reprogramming mediates GC metastasis remains elusive and demands further investigation.

Long non-coding RNAs (lncRNAs) are an important class of transcripts longer than 200 nucleotides, with no or limited protein-coding capability. They exert crucial effects to various cellular processes, including tumorigenesis and metastasis [13–15]. A host of GC-related lncRNAs have been implicated in cancer metastasis. For instance, lncRNA CCAT5 promotes GC metastasis by mediating crosstalk between STAT3 and Wnt/β-catenin pathways [16]. Another example is that lncRNA SDCBP-AS1 suppresses GC tumorigenicity and metastasis by regulating the post-translational modification of hnRNPK and destabilizing the β-catenin protein [17]. Of note, there have been several researches investigating the association between lncRNAs and FA metabolism, such as lncRNA NEAT1, which facilitates FA metabolism and lymph node metastasis through stabilization of RPRD1B and activation of c-Jun/c-Fos/SREBP1 signaling axis [18]. Nevertheless, the intricate regulatory network mediated by lncRNAs between FA metabolism and tumor metastasis requires further research.

In the current study, we identified a clinically significant lncRNA, TENM3-AS1 (Teneurin transmembrane protein 3 antisense 1), upregulated in peritoneal tumors of GC, and its high expression was strongly linked to a reduced overall survival (OS) and progression-free survival (PFS) in GC patients. Functionally, TENM3-AS1 enhanced the migratory and invasive competences of GC cells in vitro, and tumorigenesis and liver metastasis in vivo, as well as FA biosynthesis in GC cells. Mechanistically, EGR1 (Early growth response 1) stimulated the transcriptional activation of TENM3-AS1 which exerted its effects by upregulating the expression of hnRNPK (Heterogeneous nuclear ribonucleoprotein K) and FASN. Additionally, TENM3-AS1 stabilized FASN mRNA by binding with hnRNPK and increasing the deubiquitination level of hnRNPK. Our study highlights lncRNA-TENM3-AS1 as a promising novel biomarker and curative target for GC metastasis.

Materials and methods

Clinical samples obtainment and whole RNA sequencing

Human tissue samples were collected from Sun Yat-sen University Cancer Center (SYSUCC) patients in Guangzhou, China, between 2021 and 2023. The collection included four paired primary and metastatic peritoneal tumors from GC patients with peritoneal metastasis, and four primary tumors from GC patients without metastasis at diagnosis. These patients were received either palliative or radical resection. The detailed clinicopathological data of eight GC patients in the SYSUCC cohort was exhibited in Tab. S1. All patients offered informed consent for the usage of surgical specimens in the SYSUCC cohort and the Ethics Committee of SYSUCC approved this research (SZR2021-087).

Whole RNA-sequencing, including lncRNA and mRNA, was conducted by CapitalBio Technology (Beijing, China). All the procedures consisting of RNA isolation, cDNA library construction, and sequencing were executed following the manufacturer's instructions. The public databases and bioinformatical analyses included in this research were depicted in Supplementary Methods.

Culture of cell lines

Human gastric mucosal epithelial cell line GES-1 and embryo kidney cell line 293T along with all human GC cell lines (HGC27, BGC823, MKN28, AGS, MKN45, MGC803, and SGC7901) were purchased from the American Type Culture Collection (Manassas, VA, USA) and maintained pursuant to the corresponding protocols. All cells were cultured at the circumstance of 37°C with 5% CO_2, and subjected to short tandem repeat profiling and mycoplasma infection testing to authenticate the real identities without contamination before utilization.

RNA-fluorescence in situ hybridization (FISH) assay

To determine TENM3-AS1 expression in primary tumors from GC patients in the SYSUCC cohort, RNA-FISH was implemented utilizing Cy3-labled TENM3-AS1 probe (Tab. S2) and 4',6-diamidino-2-phenylindole (DAPI) solution via Fluorescent In Situ Hybridization Kit (GenePharma, Shanghai, China) as previously demonstrated [19]. Besides, RNA-FISH was used to clarify the subcellular distribution of TENM3-AS1 in GC cells, and RNA probes with Cy3-label for 18S ribosomal RNA and U6 (Tab. S2) were relatively employed to indicate the cytoplasm and nucleus. All fluorescent photographs were captured by a confocal laser scanning microscope (Carl Zeiss, Oberkochen, Germany).

RNA obtainment and real-time quantitative PCR (RT-qPCR) analysis

The total RNA extraction and reverse transcription were respectively performed with the RNA-Quick Purification Kit (ES Science, Shanghai, China) and PrimeScript™ RT Master Mix (Takara Bio Inc., Shiga, Japan) according to the instructions of manufacturer. RT-qPCR analysis was performed utilizing the TB Green Premix Ex Taq™ (Takara., Shiga, Japan) in three independent replicates on a Bio-Rad CFX96 machine [20]. Individual RNA level was expressed relative to ACTB level in each sample and calculated using the $2^{-\Delta\Delta Ct}$ method. All primer sequences exploited in RT-qPCR analyses were displayed in Tab. S3.

Western blot assay

Total protein from cell lines or animal tumor samples was extracted using SDS lysis buffer (Beyotime, Shanghai, China) with Protease and Phosphatase Inhibitor Cocktail Mix (Solarbio, Beijing, China). Total protein was separated by SDS-PAGE with electrophoresis, and transferred onto PVDF membrane (Millipore, MA, USA) for determination. Subsequently, the membrane was blocked in TBST solution mixed with 5% skim milk for 2 h, and incubated at 4℃ overnight with primary antibody as well as at room temperature for 1 h with secondary antibody. Ultimately, the membrane was visualized with a chemiluminescence substrate (Affinity, OH, USA). Tab. S4 displayed all antibodies used for Western blot assays.

Free fatty acid detection assay

The content of cellular fatty acids in GC cells was measured with Amplex Red Free Fatty Acid Assay Kit (Beyotime, Shanghai, China) pursuant to the manufacturer's protocols. 1×10^6 cells were lysed with BeyoLysis™ buffer for metabolic assay, and the supernatant was collected after centrifugation at 12,000 g for 5 min at 4℃ and transferred into a new tube. 50 uL supernatant was moved into 96-well plates and mixed with 50 uL Free fatty acid working solution, following by incubation 30 min at 37℃ in the dark. The content of cellular fatty acids was determined by detecting the absorbance of mixed liquid at 570 nm.

BODIPY staining assay

Lipid droplets in GC cells were stained via BODIPY 493/503 Staining Kit (Beyotime, Shanghai, China). The transfected GC cells were seeded onto coverslips in 24-well plates and fixed with 4% paraformaldehyde for 15 min after 24 h culture. Then, the cells were incubated with BODIPY and Hoechst staining solution for 20 min at room temperature, and washed twice with PBS. A confocal laser scanning microscope was exploited to capture images of BODIPY staining.

Oil red O staining assay

Neutral lipids were stained using Oil Red O Stain Kit (Solarbio Life Sciences, Beijing, China) in accordance with the manufacturer's instructions. The transfected cells were washed twice with PBS after removing the medium, following by fixation with the fixing solution for 30 min. Then, the cells were incubated in 60% isopropanol for 30 s and in Oil Red O staining solution for 20 min. The stain procedure was stopped with 60% isopropanol and distilled water. Next, the cells were counterstained with Mayer's Hematoxylin, and the photographs were taken via an Olympus microscope (Tokyo, Japan).

Chromatin Immunoprecipitation (ChIP) assay

To determine the specific binding sites between EGR1 and the promoter of TENM3-AS1, ChIP assay was performed by Magnetic Bead ChIP Kit (Thermofisher, MA, USA) in GC cells. The cells in 10 cm dishes were incubated with 1% formaldehyde for 10 min at room temperature to perform DNA crosslink. The crosslink reaction was terminated by glycine buffer. Next, the DNA-protein complex was digested by MNase and sonicated to obtain 200–300 bp broken chromatin. After mixing with the primary antibody at 4°C overnight, the lysates containing the digested chromatin were incubated with ChIP grade protein A/G magnetic beads at 4°C for 2 h to perform

immunoprecipitation. Subsequently, the chromatin fragments binding magnetic beads were eluted and determined by RT-qPCR and nuclear acid electrophoresis. The designed primer sequences used in ChIP assay were offered in Tab. S3.

Biotinylated RNA pull-down assay and mass spectrometry

Pierce Magnetic RNA-Protein Pull-Down Kit (Thermofisher, MA, USA) was used in RNA pull-down assay following the guidelines of manufacturer. Succinctly, the sense, anti-sense, and specific exon sequences of TENM3-AS1 were transcribed in vitro and biotinylated by MAXIscript T7 Transcription Kit (Invitrogen, CA, USA). The biotinylated RNA probe was mixed with streptavidin magnetic beads for 1 h at room temperature. Next, the magnetic beads-probe complex was incubated with total lysates of GC cells at 4°C overnight, and the bead-RNA-protein compound were thoroughly washed and resuspended with the protein lysis buffer. Furthermore, pull-down samples from immunoprecipitation were detected by SDS-PAGE with electrophoresis and the differentiated strips were collected for Mass spectrometry analysis, which was executed by Fitgene corporation (Fitgene, Guangzhou, China).

In vitro functional assays

In vitro functional assays, consisting of colony formation, wound-healing and transwell assays, were implemented in GC cells according to the detailed demonstrations in Supplementary Methods.

In vivo animal experiments

Female BALB/c nude mice ranging from 3- to 4-weeks old (Vital River, Beijing, China) were housed at the Center of Experimental Animals of SYSUCC under specific pathogen-free circumstances. The Institutional Animal Care and Use Committee of SYSUCC approved all animal experiments in this study (Protocol L102022021003Q). For xenograft tumorigenesis model, the stably transfected HGC27 cells were injected subcutaneously into the groin (5×10^6 cells; $n = 5$ for each group). Tumor volume (mm^3) was measured weekly and determined according to the formula (tumor volume = length × $width^2$ /2) as previously depicted [21]. After 28 days, all mice were euthanized by CO_2 inhalation, and the tumors were dissected and immediately weighted. The collected tumors were fixed overnight in 4% paraformaldehyde for further Hematoxylin-eosin (HE) staining and Immunohistochemistry (IHC) assays. For liver metastasis model, the stably transfected HGC27 cells with luciferase were injected into spleens of 5–6 weeks old female BALB/c nude mice (1×10^6 cells; $n = 4$ for each group). At 60 days post-injection, in vivo optical luciferase imaging assays were implemented in the mice, and the livers were dissected after mice were sacrificed. The collected livers were immediately photographed by in vivo optical luciferase imaging assays and fixed in 4% paraformaldehyde overnight for further pathological assessment. In vivo optical luciferase imaging assays was executed after intraperitoneal injection of 100 µL D-luciferin (AAT Bioquest, CA, USA) at the concentration of 15 µg/µL into mice in Xenogen IVIS Spectrum system (CA, USA) [22]. The number of metastatic foci in the liver was counted from HE staining slide.

Statistical analysis

All statistical analyses were achieved by GraphPad Prism 8 software and RStudio software (Version 4.0.2). Comparisons were conducted by two-tailed Student's *t*-test, Mann-Whitney test, one-way ANOVA test, and two-way ANOVA test in this study. Univariate Cox regression analysis was executed to clarify the clinical significance of the candidate lncRNAs in TCGA-STAD cohort. The Log-rank test was implemented to find differences of the survival probability of patients between different subgroups in Kaplan-Meier curve. The Spearman correlation test was employed to find significant genes correlated to TENM3-AS1. All experiments were completed in triplicate. The statistical results were exhibited as the mean ± standard deviation (SD) in scatter and bar plots. Statistical significance was determined as $p < 0.05$ and shown by asterisks in the figures.

Results

The clinical significance of the novel lncRNA TENM3-AS1 in GC metastasis

To identify lncRNAs playing a role in GC metastasis, we performed the whole RNA-sequencing in four paired primary (Pri group) and metastatic tumors (Pe-Met group) from four GC patients with peritoneal metastasis in the SYSUCC cohort. Compared to primary GC tumors, 708 lncRNAs were significantly upregulated, while 732 lncRNAs were downregulated in metastatic peritoneal tumors (Fig. 1A, Fig. S1A, and Tab. S5). Additionally, the transcriptome matrix and clinicopathologic data of 36 non-tumoral normal samples and 412 GC samples were retrieved from the TGCA-STAD cohort. Tumor samples were further divided into 365 M0-staged tumors (non-metastatic group; non-Met) and 29 M1-staged tumors (metastatic group; Met), excluding samples with undefined M stages. This analysis identified 228 significantly upregulated lncRNAs and 8 downregulated lncRNAs in the metastatic group compared to the non-metastatic group (Fig. 1A, Fig. S1A, and Tab. S6). After overlapping the up-regulated lncRNAs from the SYSUCC cohort and the TCGA-STAD cohorts, ten shared lncRNAs were selected for further analysis (Fig. 1A). Among these, four lncRNAs (LINC00565, TENM3-AS1, LINC00639,

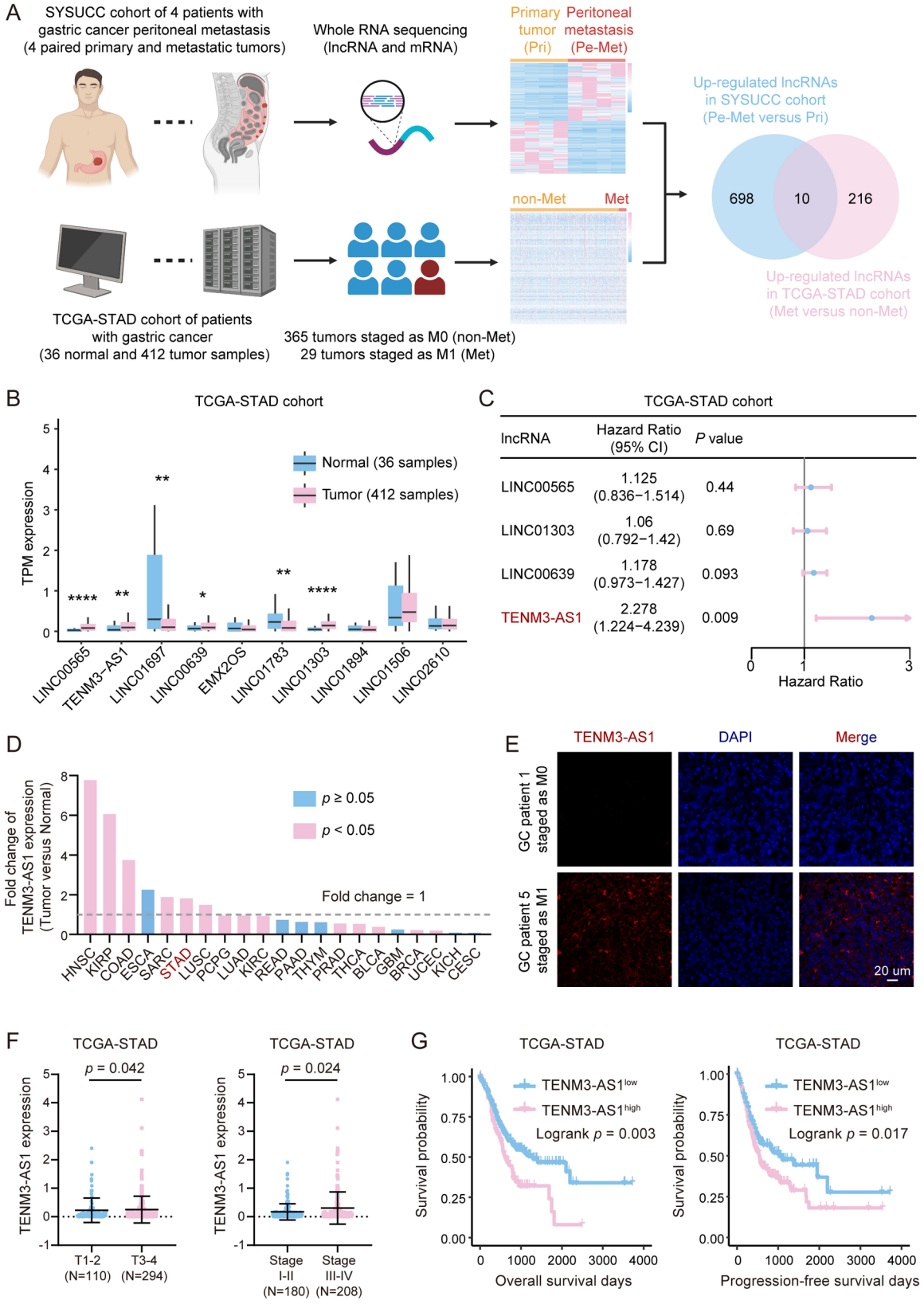

Fig. 1 (See legend on next page.)

(See figure on previous page.)

Fig. 1 Identification of the novel lncRNA TENM3-AS1 and its clinical significance to GC metastasis. (**A**) Overview of workflows to identify clinically significant lncRNAs in GC patients of the SYSUCC and the TCGA-STAD cohorts and select ten shared lncRNAs after overlapping the upregulated lncRNAs. (**B**) Expression levels of ten candidate lncRNAs in non-tumoral normal samples and GC samples in the TCGA-STAD dataset. (**C**) Univariate Cox regression analysis for overall survival based on the expression levels of four eligible lncRNAs in the TCGA-STAD cohort. (**D**) The fold changes of TENM3-AS1 expression in tumor samples versus non-tumoral normal samples across different cancer types in the TCGA database. (**E**) Representative images of RNA-FISH assays in human GC tissues from M0-staged and M1-staged patients of the SYSUCC cohort using TENM3-AS1 probe and DAPI. Scale bar means 20 μm. (**F**) Expression level of TENM3-AS1 in GC patients with low- or high-grade T stage (left) and AJCC Stage (right) from the TCGA-STAD cohort. (**G**) Kaplan-Meier curves displaying that GC patients with high expression of TENM3-AS1 gain the poor overall survival (left) and progression-free survival (right). Error bars represent mean ± SD. * means $p < 0.05$, ** means $p < 0.01$, and **** means $p < 0.0001$

and LINC01303) were significantly upregulated in GC samples from the TCGA-STAD cohort compared to non-tumoral samples, while two lncRNAs (LINC01697 and LINC01783) were significantly reduced in tumoral samples (Fig. 1B). We next performed univariate Cox regression analysis for OS of GC patients on the basis of expression of the four upregulated lncRNAs in the TCGA-STAD cohort, and identified TENM3-AS1, an antisense RNA of the Teneurin transmembrane protein 3 located on chromosome 4q34, as the only independent predictor of the impaired prognosis in GC patients (Fig. 1C).

Similar to gastric cancer (STAD), TENM3-AS1 was also significantly upregulated in other solid tumors compared to the corresponding non-tumoral tissues in the TCGA database, like head and neck cancer (HNSC), kidney papillary cell carcinoma (KIRP), colon cancer (COAD), Sarcoma (SARC), and lung squamous cell carcinoma (LUSC) (Fig. 1D). FISH assay was utilized to probe TENM3-AS1 in the primary tumors of 8 GC patients, half staged as M0 and half patients from Pe-Met group in the SYSUCC cohort. Our results revealed that TENM3-AS1 expression was markedly higher in advanced tumors compared to non-metastatic tumors (Fig. 1E). To investigate the association between TENM3-AS1 expression and various clinicopathologic factors, including T stage and American Joint Committee on Cancer (AJCC) stage, we compared TENM3-AS1 expression levels in GC patients with advanced versus lower stages. This analysis revealed a positive correlation between TENM3-AS1 expression and advanced T and AJCC stages in GC patients (Fig. 1F). In addition, high expression of TENM3-AS1 predicted the cacoethic OS and progression-free survival (PFS) in GC patients (Fig. 1G). The secondary structure of TENM3-AS1 was obtained via RNAfold software (Fig. S1B) and the coding potential of TENM3-AS1 was calculated through the CPC2 web tool and PhyloCSF software, which illustrated that TENM3-AS1 had no coding capability similar to other widely-recognized lncRNAs (Fig. S1C-D). In summary, TENM3-AS1 is shown to be predominantly elevated in metastatic or advanced tumors and correlated with a poorer prognosis in GC patients.

TENM3-AS1 is transcriptionally activated by the transcriptional factor EGR1

The expression levels of TENM3-AS1, in the human gastric mucosal epithelial cell line GES-1 and a variety of GC cell lines, were determined by RT-qPCR assay. Results demonstrated the overexpression of TENM3-AS1 in a majority of GC cell lines, in particular HGC27 and BGC823 cells (Fig. 2A), which conformed to the results above from non-tumoral samples and GC samples. In contrast, TENM3-AS1 expression was slightly changed in MKN28 cells compared to GES-1 cells (Fig. 2A). Since mRNA or lncRNA are mostly controlled by transcription factors (TFs) [23], we investigated potential TFs involved in the transcriptional activation of TENM3-AS1. Analysis of the expression levels of TFs in the SYSUCC cohort revealed 116 obviously upregulated TFs in the Pe-Met group contrasting to the Pri group (Fig. 2B and Tab. S7). We then identified candidate TFs positively correlated with TENM3-AS1, setting the criteria as Spearman's ρ value > 0.2 and p-value < 0.5 (Tab. S8). Additionally, we explored TFs potentially binding to the promoter of TENM3-AS1 using the JASPAR website (Tab. S9). After intersecting these results, 23 eligible TFs were screen out (Fig. 2C). Of note, the top ten TFs identified in the JASPAR result were considered as the highest potential regulators of TENM3-AS1 expression (Fig. 2D). Furthermore, the public single-cell RNA sequencing data of thirteen gastric antral mucosa biopsies from nine patients with non-atrophic gastritis or GC in GSE134520 dataset was acquired from GEO database. The UMAP analysis of ten aforementioned TFs revealed that only EGR1 was evidently expressed in GC cells compared to stromal or immune cells (Fig. 2E and Fig. S2A-B). The expression levels of EGR1 were compared between GC patients with M0 and M1 stage in TCGA-STAD cohort, which unfortunately showed that there was no difference of EGR1 expression between these two groups (Fig. S2C). Therefore, IHC experiments were conducted to stain EGR1 protein in primary tumor tissues from 4 GC patients staged as M0 and 4 GC patients staged as M1 in the SYSUCC cohort. The results indicated that EGR1 expression was significantly elevated in GC patients with metastatic tumors (Fig. 2F and Fig. S2D). Furthermore, EGR1 expression was increased in GC samples of higher-risk AJCC stages in the TCGA-STAD cohort when

comparing EGR1 expression between GC patients diagnosed as Stage I and II-IV (Fig. 2G). However, there was no significant difference of EGR1 expression between GC patients with Stage I-II and III-IV (Fig. S2E). High expression of EGR1 was discovered to have a detrimental impact on PFS, OS, and disease-specific survival (DSS) in GC patients (Fig. 2H and Fig. S2F). Our data showed that EGR1 actually serves as a detrimental TF in GC progression.

In addition, the certainly positive association between EGR1 and TENM3-AS1 in the TCGA-STAD dataset was drawn in Fig. 2I. The relationship was further explored in several GC cell lines using small interfering RNAs to knock down EGR1 (referred to as siEGR1 #1 and #2) and a plasmid to overexpress EGR1 (referred to as EGR1). The results demonstrated that TENM3-AS1 expression was significantly reduced alongside the downregulation of EGR1, while TENM3-AS1 expression increased in tandem with the elevated EGR1 expression (Fig. 2J and Fig. S2G). ChIP-sequencing results of H1 and Ishikawa cells using EGR1 antibody, visualized in the ENCODE database, suggested that EGR1-binding pools peaked in several sites, which were located in the promoter (2000 bp upstream from the transcription start site, namely TSS) of TENM3-AS1 (Fig. 2K). Using the JASPAR prediction tool and the validated binding motif of EGR1 (Fig. 2L), three predicted binding sites (BS1-3) were identified at 600 bp upstream from TSS in the promoter of TENM3-AS1 (Fig. 2M). Corresponding primers for different promoter segments (referred to as #1, #2, and #3) of TENM3-AS1 were synthesized for further experiments. ChIP experiments using an EGR1 antibody, along with RT-qPCR assays to validate the specific binding sites, were executed in HGC27 and BGC823 cells. The results determined that EGR1 was reproducibly bound to all the predicted sites within the promoter region of TENM3-AS1 (Fig. 2N and Fig. S2H-I). Finally, a promoter dual-luciferase reporter assay was finalized by co-transfecting 293T cells with the plasmid pEZX-FR01 containing the TENM3-AS1 promoter region, along with either siRNAs targeting EGR1 or a synthesized plasmid overexpressing EGR1. The corresponding control non-targeting siRNA and the blank vector plasmid were used as controls. Our results showed that luciferase activity was significantly declined when endogenous EGR1 expression was inhibited, whereas it was increased following exogenous EGR1 overexpression (Fig. 2O). Together our data demonstrated that EGR1 stimulates the transcriptional activation of TENM3-AS1.

TENM3-AS1 potentiates the migratory and invasive abilities of GC cells in vitro and tumor growth and liver metastasis in vivo

To explore the biological function of TENM3-AS1 in GC development and metastasis, functional assays were performed both in vitro and in vivo using HGC27 and BGC823 cells. These cells were stably transfected with short hairpin RNAs targeting TENM3-AS1 (designated as shTENM3-AS1 #1 and #2), a synthetic plasmid exogenously overexpressing TENM3-AS1 (designated as TENM3-AS1), or the corresponding controls (designated as shCtrl and Vector) (Fig. 3A and Fig. S3A). Colony formation assays confirmed that inhibiting TENM3-AS1 expression reduced the colony-forming competence of GC cells (Fig. 3B-C). In contrast, overexpressing TENM3-AS1 had the opposite effect, enhancing colony formation in GC cells (Fig. S3B-C). Similarly, wound-healing and transwell assays demonstrated that reducing TENM3-AS1 expression hindered the migratory and invasive abilities of GC cells (Fig. 3D-G), while increasing TENM3-AS1 expression enhanced the mobility of GC cells (Fig. S3D-G).

Next, we used animal experiments to investigate the role of TENM3-AS1 on GC tumor growth and metastasis in vivo. These results of subcutaneous xenograft tumor models in nude mice showed that tumors with TENM3-AS1 knockdown were significantly smaller, grew more slowly, and had reduced weights contrasting to the control group (Fig. 3H-J). In contrast, subcutaneous tumors overexpressing TENM3-AS1 exhibited faster growths and increased weights with comparison to the vector group (Fig. S3H-J). Furthermore, liver metastasis models via splenic vein injection in nude mice revealed that decreasing TENM3-AS1 expression significantly inhibited liver metastasis of GC cells and the number of the visible liver metastatic nodules decreased in shTENM3-AS1 groups when compared to the shCtrl control group (Fig. 3K-N). Conversely, overexpressing TENM3-AS1 obviously promoted liver metastasis of HGC27 cells and increased the number of the visible liver metastatic nodules (Fig. S3K-N). In a nutshell, TENM3-AS1 promotes GC cell migration and invasion in vitro, and tumorigenesis and liver metastasis in vivo.

TENM3-AS1 increases FASN expression and induces fatty acid biosynthesis in GC metastasis

To better understand the underlying mechanism by which TENM3-AS1 regulated GC metastasis, we analyzed differentially expressed genes (DEGs) by comparing RNA-sequencing data between Pri and Pe-Met groups. These studies revealed 1538 upregulated and 1443 downregulated DEGs in the Pe-Met group ($p < 0.05$ and $|\log \text{Fold change}| \geq 1$) (Fig. 4A and Tab. S7). Next, we performed functional pathways analysis via Gene Ontology

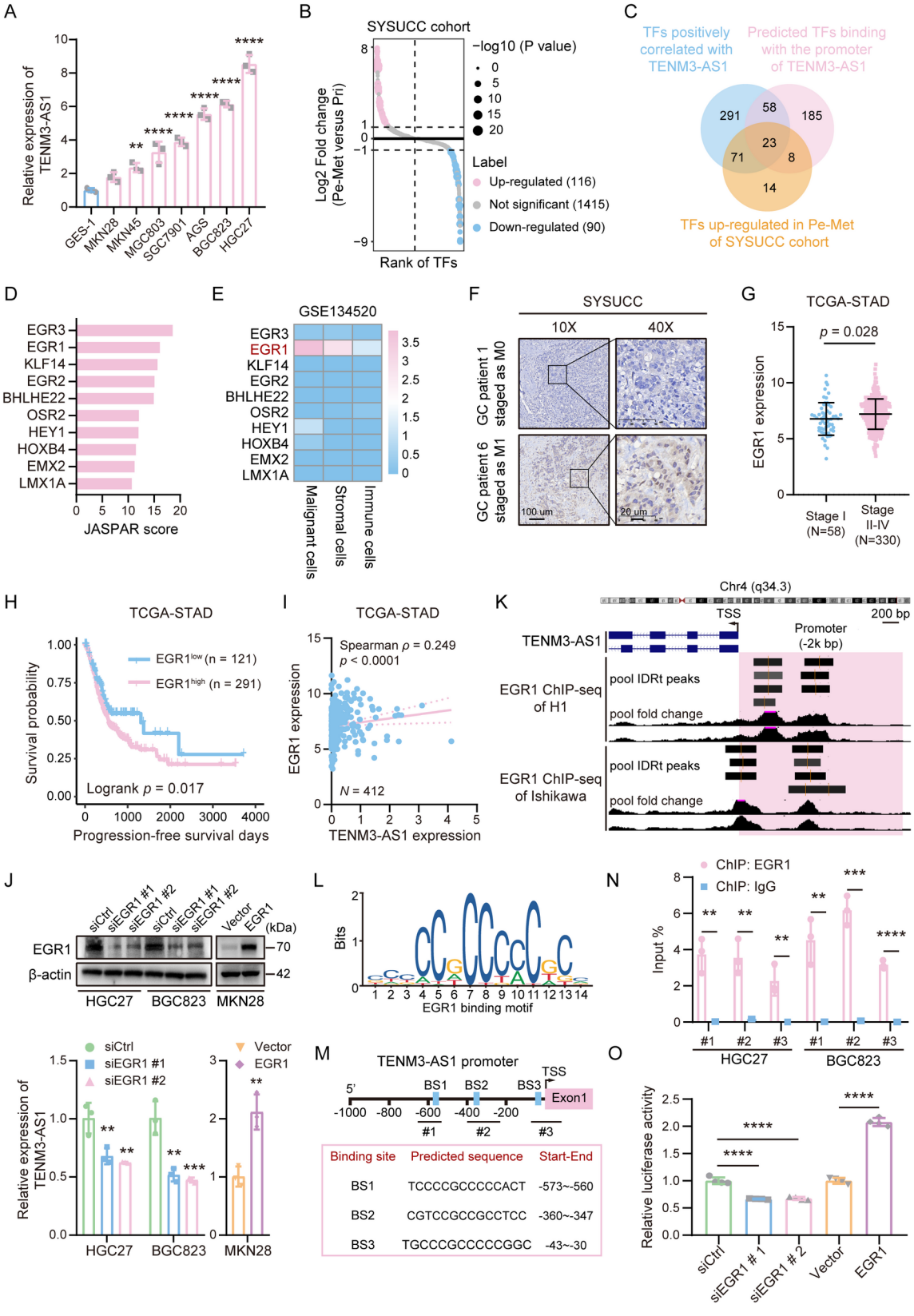

Fig. 2 (See legend on next page.)

(See figure on previous page.)

Fig. 2 TENM3-AS1 is transcriptionally regulated by EGR1. (**A**) Relative expression levels of TENM3-AS1 in GES-1 cell and GC cell lines. (**B**) Volcano plot showing the differently expressed TFs in metastatic tumors versus primary tumors in mRNA-sequencing data of the SYSUCC cohort. (**C**) Venn diagram to identify the potential TFs modulating TENM3-AS1 transcription. (**D**) Binding probability predicted in JASPAR database to find the highest-potential TFs. (**E**) Heatmap displaying expression levels of ten eligible TFs in malignant, stromal, and immune cells of GSE134520 dataset. (**F**) Representative images of IHC assays in human GC tissues from M0-staged and M1-staged patients of the SYSUCC cohort to indicate EGR1 expression. The scale bar means 100 μm in 10X field and 20 μm in 40X field. (**G**) Expression levels of EGR1 in GC patients with the low- or high-grade AJCC stage in TCGA-STAD cohort. (**H**) Kaplan-Meier curve showing GC patients with high expression of EGR1 attain a worse progression-free survival in TCGA-STAD cohort. (**I**) Correlation of TENM3-AS1 and EGR1 expression levels in TCGA-STAD cohort. (**J**) Validation of knocking down or overexpressing EGR1 in GC cells (top), and the corresponding relative expression changes of TENM3-AS1 (bottom). (**K**) ChIP-sequencing result from ENCODE database verifying EGR1 binds with the promoter region of TENM3-AS1 in H1 and Ishikawa cells. (**L**) The validated binding motif of EGR1. (**M**) The predicted binding sites (BS1-3) of EGR1 on the promoter of TENM3-AS1 and the designed fragments (#1, #2, and #3) for further ChIP analysis. (**N**) Result of ChIP assays using antibodies against EGR1 and IgG in GC cells. (**O**) Result of promoter dual-luciferase reporter assay performed by co-transfecting 293T cells with the plasmid pEZX-FR01 containing the TENM3-AS1 promoter region, along with either siRNAs targeting EGR1 or a synthesized plasmid overexpressing EGR1. Error bars represent mean ± SD. ** means $p < 0.01$, *** means $p < 0.001$, and **** means $p < 0.0001$

Biological Process (GO-BP) and Kyoto Encyclopedia of Genes and Genomes (KEGG) databases in DAVID website. Results demonstrated that a series of metabolic processes were critical for GC metastasis formation, especially fatty acid (FA) metabolism (Fig. 4B-C). Among the processes of FA metabolism, including biosynthesis, transport, catabolism, and oxidation of FA, only the biosynthetic process of FA was significantly increased in GC patients with high expression of TENM3-AS1 in the TCGA-STAD cohort (Fig. 4D and Fig. S4A). To test whether TENM3-AS1 participated in the modulation of FA metabolism, the total content of cellular FAs was measured, revealing that silencing TENM3-AS1 significantly reduced cellular FA levels, while overexpressing TENM3-AS1 led to a marked increase in FA accumulation (Fig. 4E). Additionally, intracellular lipid droplets stained with the lipophilic fluorescent dye BODIPY 493/503 and Oil Red O demonstrated that lower TENM3-AS1 expression inhibited lipid storage, whereas higher TENM3-AS1 expression was associated with lipid accumulation in GC cells (Fig. 4F-I).

To identify FA biosynthesis-related genes potentially regulated by TENM3-AS1, genes that positively correlated with TENM3-AS1 (Tab. S8), genes upregulated in the Pe-Met group of the SYSUCC cohort (Tab. S7), and genes involved in the FA biosynthetic process (GO: 0006633) were intersected. This analysis revealed ten key genes (Fig. 4J), among which FASN appeared to be the most promising candidate. Previous study identified that FASN catalyzed the transformation of acetyl-CoA and malonyl-CoA into palmitate and other long-chain saturated FAs, which was linked to GC progression and metastasis [24]. To unveil how TENM3-AS1 influenced FA biosynthesis, we examined the expression levels of pivotal genes related to FA biosynthesis (FASN and SCD1), β-oxidation (CPT1A), and lipid transport (CD36) in GC cells. Our results indicated that TENM3-AS1 knockdown was correlated with the reduced mRNA and protein expression levels of FASN and SCD1, while minimal impact on CPT1A and CD36 expression was observed (Fig. 4K-L and Fig. S4B-D). Conversely, overexpression of TENM3-AS1 was associated with an increased expression of FASN and SCD1 at both mRNA and protein levels, while CPT1A and CD36 levels remained unaffected (Fig. 4K-L and Fig. S4B-D). Collectively, TENM3-AS1 enhances FA biosynthesis and accumulation in GC metastasis in part by upregulating FASN expression.

TENM3-AS1 promotes GC migration and invasiveness via interacting with hnRNPK and enhancing its deubiquitination

It is well accepted that the function of lncRNAs depends upon the proper subcellular localization. Subcellular fractionation assays and RT-qPCR experiments, along with RNA-FISH analysis in GC cells demonstrated that TENM3-AS1 was predominantly localized in the cytoplasm (Fig. 5A-B). On the basis of the results suggesting a regulatory relationship between TENM3-AS1 and FASN, a RIP assay using an anti-FASN antibody was performed but unexpectedly revealed that TENM3-AS1 did not directly interact with the FASN protein (Fig. S4E). To identify potential candidates that might be involved in TENM3-AS1 regulation of FASN, we performed an RNA pull-down assay and Mass Spectrometry (MS) analysis comparing the biotin-labeled TENM3-AS1 sense probe and the control anti-sense probe (Fig. 5C). Among the proteins pulled down by TENM3-AS1, we identified hnRNPK (Fig. 5D), an RNA-binding protein relevant to GC progression [25]. Interaction between TENM3-AS1 RNA and hnRNPK protein was verified by RNA pull-down assay and Western blot experiment (Fig. 5E) as well as in vitro RIP assay in GC cells (Fig. 5F and Fig. S4F). To delineate the region(s) of TENM3-AS1 responsible for interacting with hnRNPK, RNA pull-down assays using various exon probes labeled by biotin spanning TENM3-AS1 sense sequences were performed. These studies showed that the exon 5 segment of TENM3-AS1 was involved in hnRNPK binding (Fig. 5G). Previous studies have shown that the K homology (KH) domains of hnRNPK, consisting of KH1, KH2, and KH3, are crucial for its RNA-binding activity [26]. Meanwhile, the

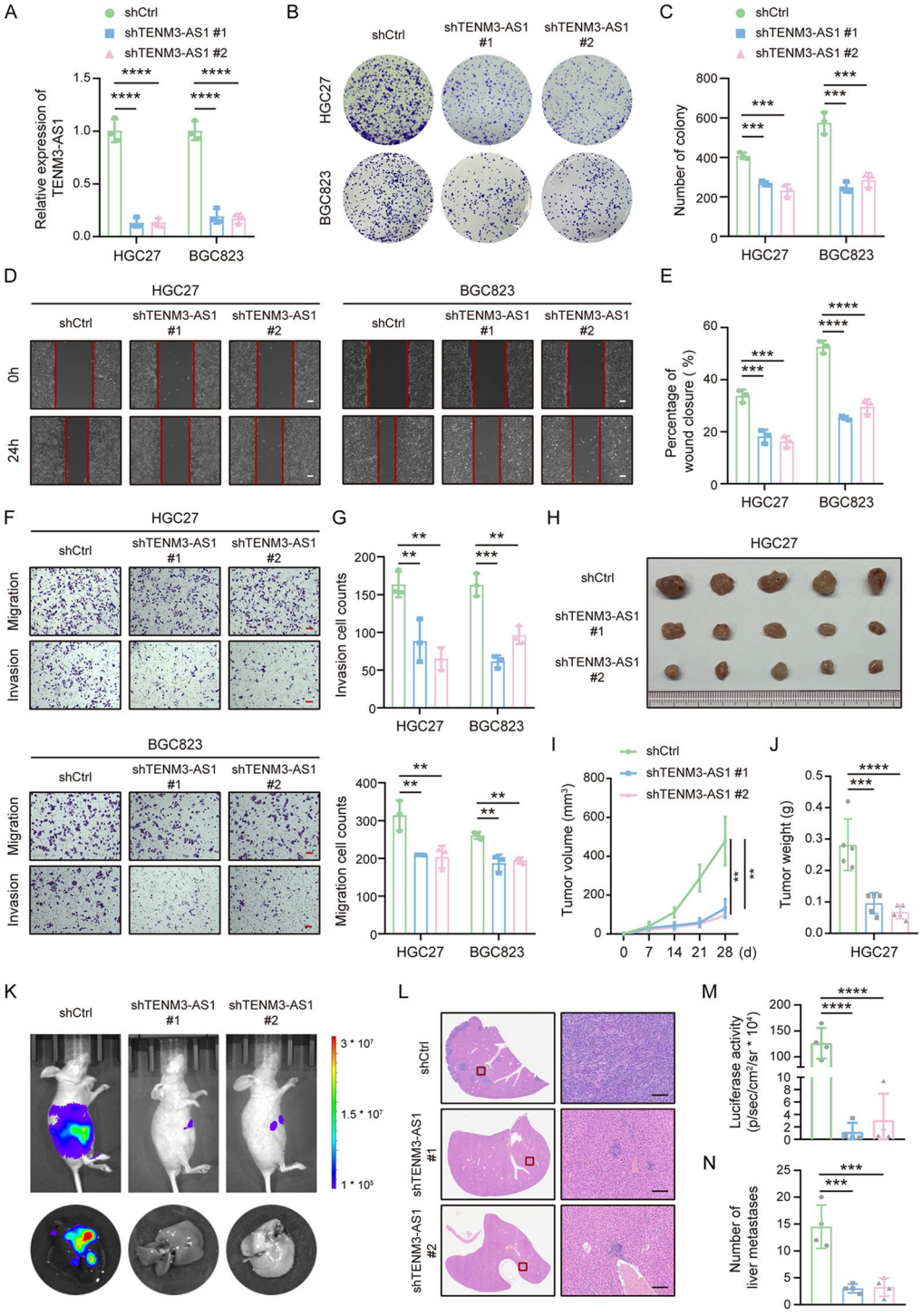

Fig. 3 TENM3-AS1 knockdown curbs the migration and invasiveness of GC cells in vitro and tumorigenesis and liver metastasis in vivo. (**A**) RT-qPCR result displaying the relative TENM3-AS1 expression after stably knocking down TENM3-AS1 by shRNAs in GC cells. (**B-C**) Representative graphs (**B**) and quantitative data (**C**) of colony formation assays in GC cells stably down-regulating TENM3-AS1. (**D-E**) Representative graphs (**D**) and quantitative data (**E**) of wound-healing assays in GC cells stably decreasing TENM3-AS1 expression. (**F-G**) Representative graphs (**F**) and quantitative data (**G**) of transwell assays in GC cells stably down-regulating TENM3-AS1. (**H-J**) Representative images of xenograft tumors morphology (**H**), quantitative data of tumors growth (**I**), and weights of xenograft tumors (**J**) in nude mice (5 mice per group) injected subcutaneously into groin region using the stably transfected GC cells. (**K**) Representative images of optical luciferase imaging assays in vivo in mouse models with liver metastasis. (**L**) HE staining assay showing the metastatic nodules in livers. (**M-N**) Quantitative data of in vivo optical luciferase imaging assays (**M**) and metastatic foci in liver tissues (**N**). Scale bars in this figure all signify 100 μm. Error bars represent mean ± SD. ** means $p < 0.01$, *** means $p < 0.001$, and **** means $p < 0.0001$

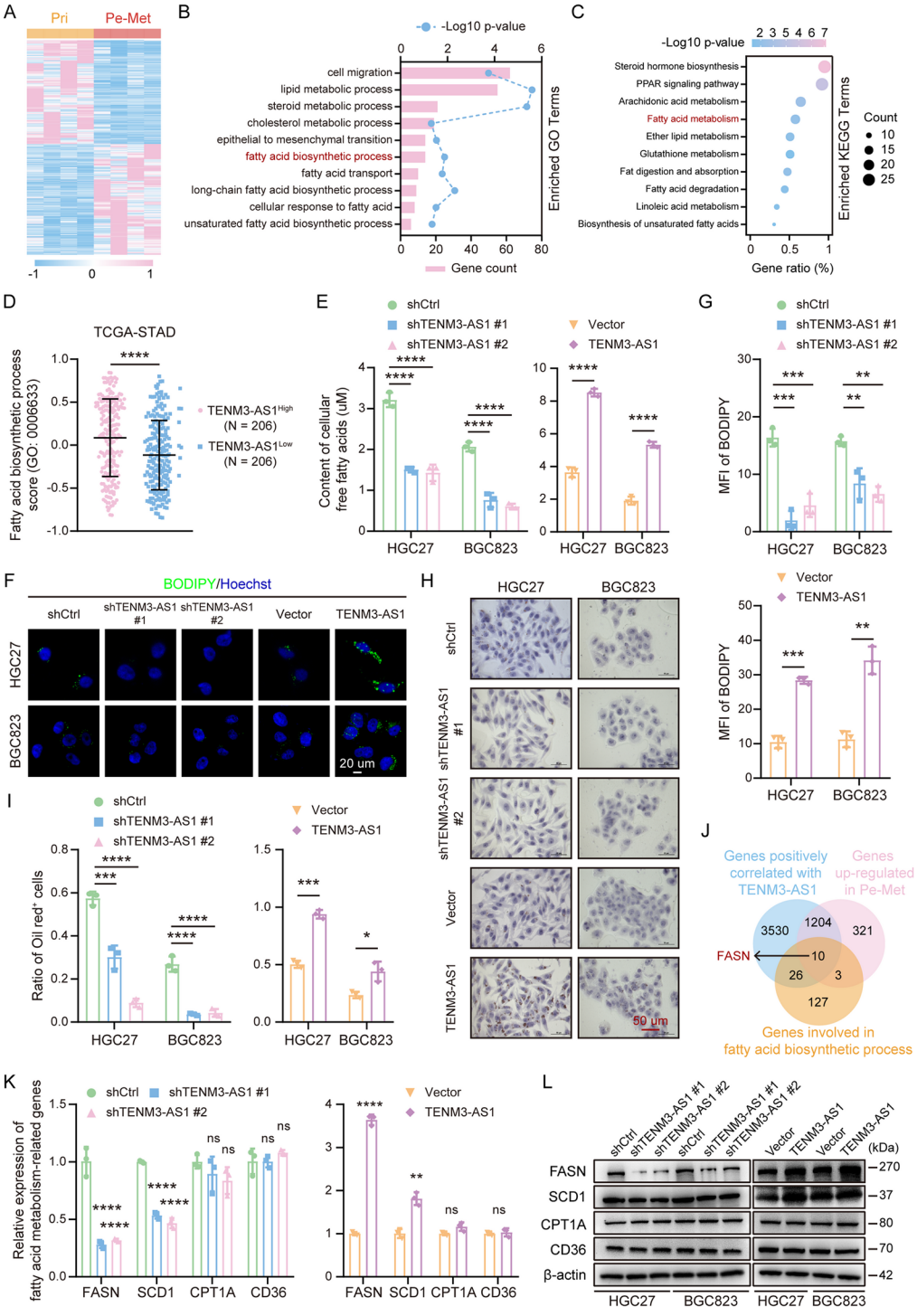

Fig. 4 TENM3-AS1 promotes fatty acid biosynthesis by increasing FASN in GC metastasis. (**A**) Heatmap exhibiting the differently expressed genes (DEGs) in metastatic (Pe-Met) and primary (Pri) tumors in the SYSUCC cohort. (**B-C**) Functional enrichment assays using GO-BP (**B**) and KEGG (**C**) pathways based on the DEGs in the SYSUCC cohort. (**D**) GSVA score of FA biosynthetic process in GC patients with high- or low-expression of TENM3-AS1 in TCGA-STAD cohort. (**E**) Quantitative data of FA detection assays in GC cells stably knocking down TENM3-AS1 (left) or overexpressing TENM3-AS1 (right). (**F-G**) Representative images (**F**) and statistical data (**G**) of BODIPY staining assays. The scale bar indicates 20 μm. (**H-I**) Representative images (H) and statistical data (**I**) of Oil Red O staining assays. The scale bar indicates 50 μm. (**J**) Venn diagram identifying the FA-biosynthesis-process-related gene potentially influenced by TENM3-AS1. (**K**) RT-qPCR result revealing the relative RNA expression of FASN, SCD1, CPT1A, and CD36 in stably transfected HGC27 cells. (**L**) Result of Western blot experiments performed in stably transfected GC cells to validate protein expression of FASN, SCD1, CPT1A, and CD36. Error bars represent mean ± SD. ns means not significant, * means $p < 0.05$, ** means $p < 0.01$, *** means $p < 0.001$, and **** means $p < 0.0001$

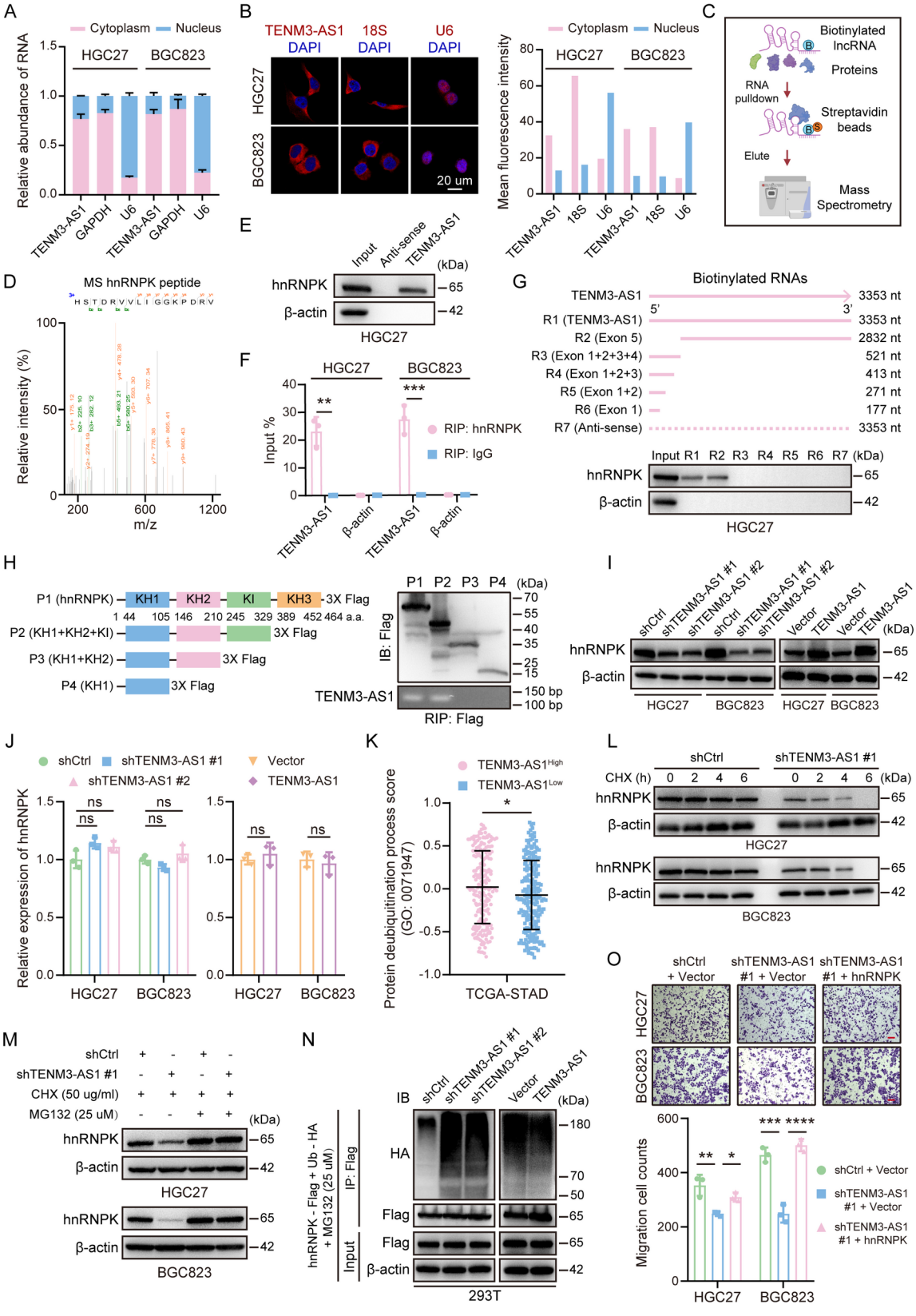

Fig. 5 (See legend on next page.)

(See figure on previous page.)

Fig. 5 TENM3-AS1 interacts with RNA-binding protein hnRNPK and increases its deubiquitination in GC cells. (**A**) Subcellular fractionation assays revealing the relative abundance of TENM3-AS1 in cytoplasm and nucleus of GC cells. GAPDH and U6 are employed as indicators for the cytoplasmic and nuclear region, respectively. (**B**) Representative images (left) and statistical data (right) of RNA-FISH assays using TENM3-AS1, 18S ribosomal RNA, and U6 probes. 18S ribosomal RNA and U6 are used as positive controls for cytoplasm and nucleus, respectively. The scale bar symbolizes 20 μm. (**C**) Schematic workflow of the biotinylated RNA pull-down assay and Mass spectrometry to clarify TENM3-AS1-binding proteins. (**D**) Representative hnRNPK peptides binding with TENM3-AS1 detected by Mass spectrometry. (**E-F**) Result of RNA pull-down analysis (**E**) and RIP assay (**F**) validating the interaction between TENM3-AS1 and hnRNPK. (**G**) Schematic diagram of full-length sense or anti-sense and specific exons fragments spanning TENM3-AS1 (top) and result of RNA pull-down analysis using different biotinylated RNA fragments in HGC27 cell (bottom). (**H**) Schematic diagram of full domains and constructed truncations of hnRNPK (left), validation of biosynthesized Flag-tagged plasmids with various truncations of hnRNPK (right and top) and result of RIP assay using antibody against Flag in HGC27 cell (right and bottom). (**I**) Western blot experiment revealing the protein expression of hnRNPK following TENM3-AS1 knockdown or overexpression. (**J**) RT-qPCR assay indicating the RNA expression of hnRNPK in GC cells diminishing or increasing TENM3-AS1 expression. (**K**) GSVA score of protein deubiquitination process in GC patients with high- or low-expression of TENM3-AS1 in the TCGA-STAD cohort. (**L**) Result of CHX-chase assay to observe the protein stabilization of hnRNPK in GC cells stably knocking down TENM3-AS1 using cycloheximide (CHX, 50 ug/mL) treatment at different time. (**M**) Western blot experiments to detect hnRNPK protein in stably transfected GC cells treated with CHX at 6 h and with or without MG132 (25 μM). (**N**) Result of in vitro ubiquitination assay revealing hnRNPK deubiquitination in 293T cell. (**O**) Representative images (top) and statistical data (bottom) of rescued transwell assay for migration in GC cells. Scale bars symbolize 100 μm. Error bars represent mean ± SD. ns means not significant, * means $p < 0.05$, ** means $p < 0.01$, *** means $p < 0.001$, and **** means $p < 0.0001$

K interactive (KI) domain, located between KH2 and KH3, plays an intricate role in modulating RNA-protein interactions [27]. We constructed several Flag-tagged plasmids with various truncations of hnRNPK and performed in vitro RIP assays. Our studies confirmed that hnRNPK interacted with TENM3-AS1 through the KI domain (Fig. 5H and Fig. S4G).

Furthermore, Western blot and RT-qPCR analyses illuminated that TENM3-AS1 knockdown reduced the expression of hnRNPK at the protein level, while overexpression of TENM3-AS1 increased hnRNPK protein expression, without significantly affecting its mRNA expression (Fig. 5I-J and S4H). Studies have shown that lncRNA can modulate protein expression through post-translational modification such as ubiquitination [28]. Next, we performed GSVA analysis using GO-BP gene sets and found that the protein deubiquitination process was enriched in GC patients with high expression of TENM3-AS1 in the TCGA-STAD cohort (Fig. 5K). We hypothesized that TENM3-AS1 might increase hnRNPK protein expression by enhancing its deubiquitination. CHX-chase assay and treatment with MG132 confirmed that TENM3-AS1 knockdown led to destabilization of the hnRNPK protein, resulting in an increased degradation rate in GC cells (Fig. 5L-M and S4I-J). An in vitro ubiquitination assay showed that hnRNPK ubiquitination was increased along with TENM3-AS1 knockdown, whereas TENM3-AS1 overexpression was associated with reduced hnRNPK ubiquitination (Fig. 5N and S4K). These results suggested that TENM3-AS1 upregulated hnRNPK protein expression by facilitating hnRNPK deubiquitination and increasing protein half-life. To further investigate whether TENM3-AS1 promoted GC progression via its interaction with hnRNPK, we performed rescue experiments by simultaneously knocking down TENM3-AS1 and exogenously upregulating hnRNPK in GC cells. These studies revealed that hnRNPK could restore the reduced migratory and invasive capabilities caused by TENM3-AS1 knockdown (Fig. 5O and Fig. S5A-B). Likewise, in vivo rescue experiments of liver metastasis models unraveled that exogenously overexpressing hnRNPK reinforced the restrained ability to metastasize to the liver triggered by TENM3-AS1 knockdown in GC cells (Fig. S5C-D). Overall, these data demonstrated that TENM3-AS1 interacts with hnRNPK to enhance its deubiquitination, thereby increasing hnRNPK protein levels and promoting GC progression.

Activation of the TENM3-AS1/hnRNPK/FASN axis reprograms fatty acid metabolism

It has been widely recognized that RNA-binding proteins exerts important effects to stabilize RNA [29–31], which prompted us to test whether TENM3-AS1 might increase FASN expression through hnRNPK-mediated mRNA stabilization. Results of eCLIP-sequencing with hnRNPK antibody in HepG2 cells derived from the ENCODE database suggested that hnRNPK probably bound to FASN mRNA (Fig. 6A). Indeed, RNA pull-down and RIP assays confirmed the interaction between hnRNPK protein and FASN mRNA (Fig. 6B-C and Fig. S6A). Next, RT-qPCR analysis manifested that mRNA expression of FASN was noticeably reduced after hnRNPK knockdown by siRNAs, while its expression was elevated when exogenous hnRNPK was overexpressed in HGC27 cells (Fig. 6D). Furthermore, RNA stabilization assay using actinomycin D (Act-D) demonstrated that hnRNPK knockdown significantly decreased the half-life of FASN mRNA (2.846 h versus 0.753 h and 1.333 h), whereas hnRNPK overexpression prolonged its half-life in HGC27 cell (2.391 h versus 2.930 h) (Fig. 6E). Rescue expression experiments using shTENM3-AS1 #1 and an hnRNPK-overexpressing plasmid demonstrated that overexpression of hnRNPK effectively restored the mRNA and protein expression of FASN caused by TENM3-AS1 knockdown (Fig. 6F-G). Interestingly, the reduced half-life of FASN mRNA induced by TENM3-AS1 knockdown was significantly

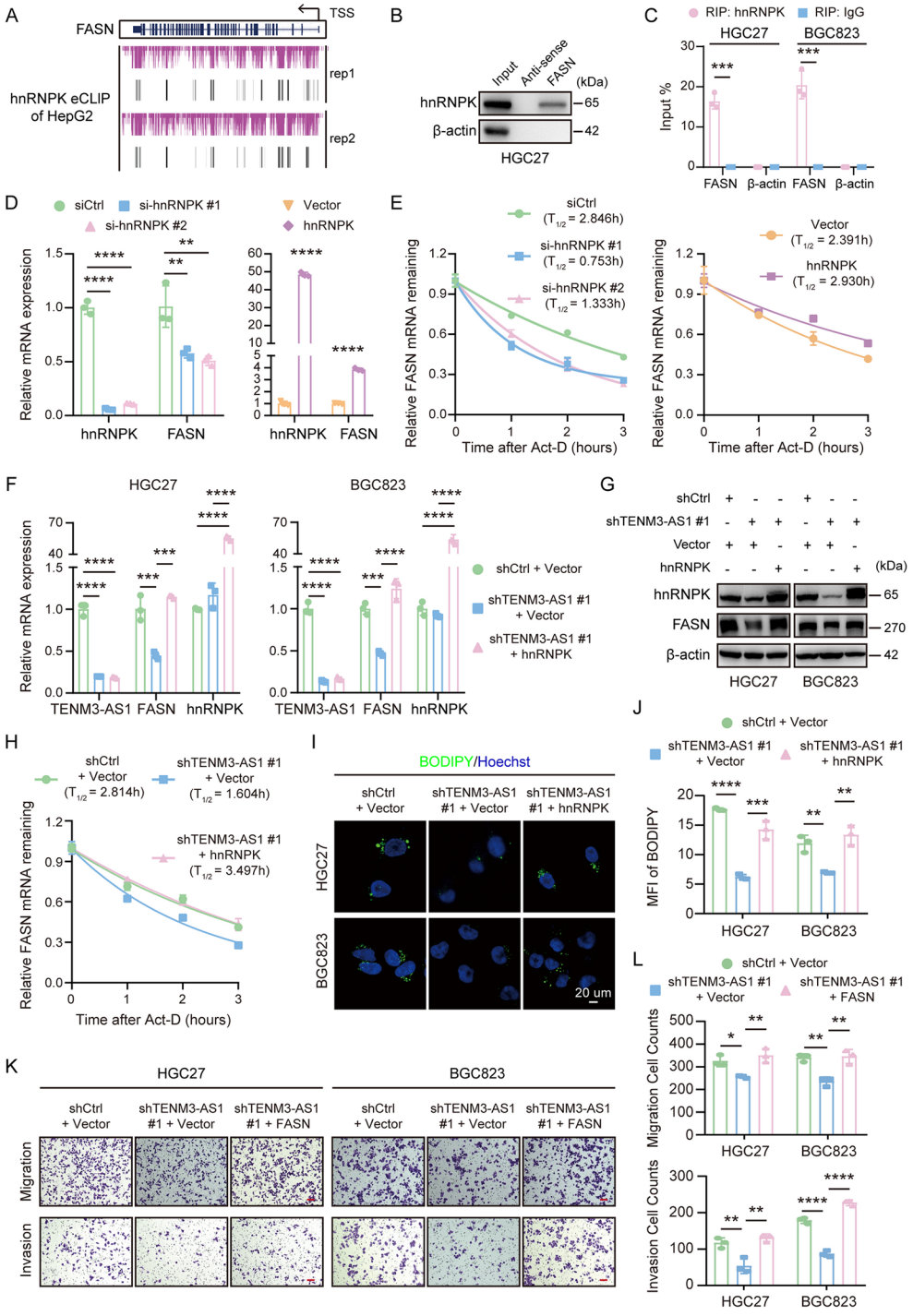

Fig. 6 TENM3-AS1 reprograms FA metabolism via hnRNPK-stabilized FASN mRNA. (**A**) eCLIP-sequencing result from ENCODE database validating the combination of anti-hnRNPK protein and FASN mRNA in HepG2 cell. (**B-C**) Results of RNA pull-down assay using sense and anti-sense probes of FASN (**B**) and RIP assay using anti-hnRNPK or IgG antibodies (**C**) confirming the interaction between hnRNPK protein and FASN mRNA. (**D**) RT-qPCR result unraveling the relative RNA expression levels of hnRNPK and FASN in GC cells knocking down (left) or upregulating (right) hnRNPK. (**E**) Result of RNA stabilization assay in transiently transfected HGC27 cell with 5 μg/mL actinomycin D (Act-D) treatment at different times to examine RNA stabilization of FASN. (**F-G**) Results of rescued RT-qPCR experiment (**F**) and Western blot assay (**G**) by co-transfecting GC cells with shRNA targeting TENM3-AS1 and a hnRNPK plasmid to observe the expression levels of TENM3-AS1, FASN, and hnRNPK. (**H**) Rescued RNA stabilization assay validating RNA stabilization of FASN in co-transfected HGC27 cell. (**I-J**) Representative images (**I**) and statistical data (**J**) of rescued BODIPY staining assay in GC cells. Scale bar means 20 μm. (**K-L**) Representative images (**K**) and statistical data (**L**) of rescued transwell assays for migration and invasion performed in GC cells co-infecting shRNA targeting TENM3-AS1 and a FASN plasmid. Scale bars represent 100 μm. Error bars represent mean ± SD. * means $p < 0.05$, ** means $p < 0.01$, *** means $p < 0.001$, and **** means $p < 0.0001$

extended by hnRNPK overexpression (Fig. 6H). Additionally, we performed Western blot assays to assess the protein expression levels of hnRNPK and FASN in metastatic tumors from in vivo rescue experiments executed in Fig. S5C-D, which showed that hnRNPK overexpression rescued the attenuated expression of FASN generated by TENM3-AS1 knockdown (Fig. S6B). Furthermore, TENM3-AS1 knockdown led to a reduction in FA storage, which was rescued by overexpressing hnRNPK in GC cells (Fig. 6I-J). To confirm whether FASN participated in the regulatory process of TENM3-AS1-induced GC cells migratory functions, rescue experiments were conducted by co-transfecting shTENM3-AS1 #1 with a plasmid overexpressing FASN. The results revealed that FASN overexpression restored the migratory and invasive capabilities of GC cells, whereas TENM3-AS1 knockdown had the opposite effect (Fig. 6K-L and Fig. S6C). To summarize, TENM3-AS1 rewires FA metabolism and intensifies the aggressiveness of GC cells by hnRNPK-stabilized FASN mRNA and the following upregulation of FASN.

TENM3-AS1/hnRNPK/FASN axis plays a significant role in GC metastasis

To disclose the clinical significance of hnRNPK and FASN, we compared their expression between non-tumoral and GC samples in TCGA-STAD. Our analysis revealed that both hnRNPK and FASN were considerably upregulated in GC samples when compared to non-tumoral samples (Fig. 7A). Importantly, high expression of FASN predicted a worsened OS and the shortened time to first progression in GC patients (Fig. 7B). However, the expression of hnRNPK was not significantly associated with the prognosis of GC patients (Fig. S6D). Additionally, IHC experiments in the SYSUCC cohort including 4 non-metastatic and 4 metastatic gastric tumors revealed that hnRNPK and FASN proteins were increased in the metastatic GC tissues, which coincided with high expression of TENM3-AS1 (Fig. 7C). Besides, the expression levels of FASN and hnRNPK were compared between GC patients with M0 and M1 stage in TCGA-STAD cohort, which showed that there was negligible difference of FASN and hnRNPK expression between two groups (Fig. S6E). To confirm the importance of the TENM3-AS1/hnRNPK/FASN regulatory axis in vivo, additional IHC experiments were conducted on xenograft tumor samples described in the Fig. 3F model. The results illuminated that hnRNPK and FASN protein levels were significantly diminished in the shTENM3-AS1 group compared to the control group (Fig. 7D), consistent with the in vitro findings. Ultimately, the proposed mechanism of TENM3-AS1 in gastric cancer (GC) metastasis is illustrated in the schematic diagram in Fig. 7E. This model depicts that the EGR1/TENM3-AS1/hnRNPK/FASN signaling axis can serve as a novel curative target for metastatic GC.

Discussion

Growing evidence suggests that lncRNAs are the essential modulatory factors in tumorigenesis and cancer metastasis [32]. There have been several phase I/II clinical trials targeting lncRNAs [33]. Although several lncRNAs relevant to GC progression and metastasis have been investigated, there is still an important need for clinically significant lncRNAs. In this study, by comparing lncRNA sequencing data from paired primary and peritoneal metastatic tumors in the SYSUCC cohort, along with the public transcriptome data from non-metastatic and metastatic samples in the TCGA-STAD cohort, we identified a novel lncRNA, TENM3-AS1. This lncRNA was aberrantly activated in metastatic and advanced primary tumors and was strongly associated with the shorter OS and PFS. Notably, this study is the first to investigate TENM3-AS1 in tumor progression. TENM3-AS1 is the antisense RNA of TENM3, a gene recognized as a significantly mutated driver with prognostic importance in esophageal squamous cell carcinoma [34]. Furthermore, functional experiments revealed that TENM3-AS1 stimulates the migratory and invasive capacity of GC cells in vitro and tumor growth and liver metastasis in vivo.

It is widely understood that TF strongly contributes to regulating RNA expression, including lncRNAs, by binding to promoters [35]. For instance, EGR1 increases the transcription of lncRNA HNF1A-AS1 and LINC01503 and thereby promotes the cell-cycle progression in GC [36, 37]; TEAD4 transcriptionally regulates lncRNA MNX1-AS1 to potentiate GC progression via inhibition of BTG2 and activation of BCL2 expression [38]; FOXO1 activates lncRNA LYPLAL1-DT to prevent triple-negative breast cancer aggressiveness via restricting abnormal Wnt/β-catenin signaling [20]. Our data uncovered that EGR1 transcriptionally regulates TENM3-AS1 expression. Previous researches have shown that EGR1 is upregulated in various tumors and promoted cancer progression and metastasis, including in GC [39–41]. These are in agreement with our findings, which reveals its role in promoting metastasis and its negative clinical impact in GC. Though the results of comparing EGR1 expression between GC patients with M0 and M1 stage, as well as Stage I-II and III-IV in TCGA-STAD cohort, showed the insignificant association, several previous studies have detected the positive correlation between EGR1 expression and the clinical stages of GC patients. For instance, the protein and transcript expression levels of EGR1 in 115 GC patients are evaluated, which hints that the cytoplasmic or nuclear expression of EGR1 and its transcripts in GC are positively correlated with tumor infiltration, lymph node and distant metastasis, as well as

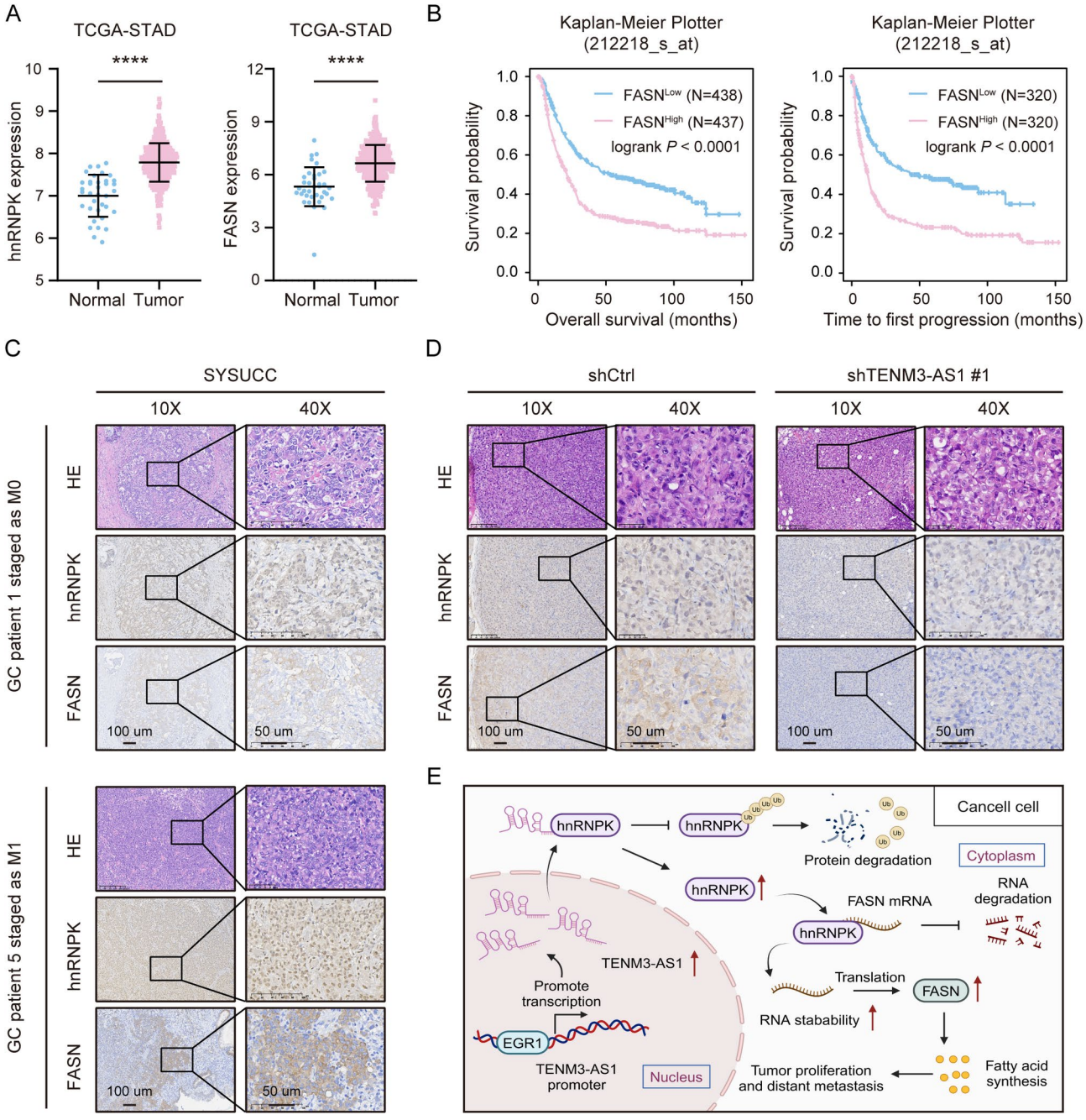

Fig. 7 Verification of clinical significance of TENM3-AS1/hnRNPK/FASN axis in GC metastasis. (**A**) Expression levels of hnRNPK (left) and FASN (right) in non-tumoral normal samples and GC samples in the TCGA-STAD dataset. (**B**) Kaplan-Meier curves illustrating that GC patients with high expression of FASN have a poor overall survival (left) and the shortened time to first progression (right). (**C-D**) Representative images of HE and IHC assays in human GC tissues from M0-staged and M1-staged patients of the SYSUCC cohort (**C**) and in xenograft tumors from Fig. 3F (**D**) to show hnRNPK and FASN expressions. The scale bar means 100 μm in 10X field and 50 μm in 40X field. (**E**) Schematic view demonstrating the functional role and regulatory mechanisms of TENM3-AS1 in reprogramming FA metabolism and promoting GC metastasis. Error bars represent mean ± SD. **** means $p < 0.0001$

AJCC stages [42]; another study tests the EGR1 protein immunohistochemically in tissue blocks attained from 140 GC patients, and unravels that EGR1 expression is positively correlated to tumor size, depth of invasion, lymph node metastasis, and AJCC stage [43]. In a nutshell, the correlations between EGR1 expression and the clinicopathological parameters need more explorations in GC patient cohorts with more samples in the future.

Further, mRNA sequencing and FA metabolism-related experiments, including BODIPY and Oil Red O staining as well as measurements of total FA content, revealed that TENM3-AS1 primarily influences FA biosynthesis in

GC cells by promoting the mRNA and protein expression of FA biosynthesis-related gene FASN. Abnormal metabolic rewiring has been regarded as one of the cancer hallmarks, among which FA metabolism enables cancer cells to exploit excess FAs to meet the need for nutrients, cellular organelles, and membrane construction, unlimited proliferation, survival during metastatic process, and activation of essential signaling pathways [44, 45]. Specifically, FASN acts as the key rate-limiting lipogenic enzyme, driving the final catalytic step of FA biosynthesis, which is essential for tumorigenesis and metastasis [46, 47]. Likewise, SCD1 is responsible for FA desaturation as a key enzyme of FA biosynthesis and induced drug resistance and self-renewal in GC [48]. It also promotes invasion and metastasis in hepatocellular carcinoma through a mechanoresponsive pathway and lipid metabolic reprogramming [49]. Regarding the interplay between lncRNAs and FA metabolism, POU6F2-AS1 reprograms FA metabolism and promotes colorectal cancer growth by upregulating FASN [50]; lncRNA ROPM influences FA metabolism, thereby enhancing breast cancer stemness [51]; and LINC00924 induces FA metabolic rewiring, facilitating GC peritoneal metastasis through interaction with hnRNPC/Mnk2 [52]. Therefore, understanding the modulatory relationship between TENM3-AS1 and FA metabolism contributes to better therapeutically targeting the vulnerability of GC metastasis.

Additionally, RIP assays revealed that TENM3-AS1 could not bind with FASN protein directly. RNA-pull down, Mass spectrometry analysis and RIP assays demonstrated that TENM3-AS1 bound with hnRNPK directly. The binding site was identified as the exon 5 of TENM3-AS1 and the KI domain of hnRNPK. Furthermore, we showed that TENM3-AS1 stabilized hnRNPK protein and elevated its expression by promoting its deubiquitination reducing its degradation rate. Similarly, lncRNA PSTAR activates p53 signaling by interacting with hnRNPK and inhibiting its deSUMOylation, thereby suppressing hepatocellular carcinoma [53]. lncRNA LYPLAL1-DT interacts with hnRNPK, influencing its cytoplasmic-nuclear shuttling without affecting its overall expression [20]. Additionally, lncRNA pancEts-1 interacts with hnRNPK and mediated β-catenin protein stabilization, thereby promoting neuroblastoma progression [54]. Additional rescue expression and functional experiments highlighted that TENM3-AS1 reprogrammed FA metabolism and mediated GC metastasis via interaction between hnRNPK and FASN, as well as hnRNPK-stabilized FASN transcript. Collectively, the TENM3-AS1/hnRNPK/FASN axis acts as a pro-metastatic pathway in GC.

Although the overexpression levels of TENM3-AS1, EGR1, hnRNPK, and FASN have been validated in primary tumors from GC patients with either non-metastatic or metastatic tumor burden in the SYSUCC cohort, further confirmation in a larger cohort of GC patients is needed due to the insignificant comparison of EGR1, hnRNPK, and FASN between GC patients diagnosed as M0 and M1 stage in TCGA-STAD cohort. And the prognostic value of hnRNPK expression in GC patients should be explored in future studies. Besides, the sequencing data from TENM3-AS1 up- or down-regulated tumors should be supplemented in the future to directly validate the underlying mechanism by which TENM3-AS1 modulated GC metastasis. Additionally, the precise molecular mechanism by which TENM3-AS1 influences the deubiquitination level of hnRNPK warrants future studies.

Conclusions

The present study identifies the pro-metastatic lncRNA TENM3-AS1 in GC cohorts, which is abnormally activated in metastatic tumors driven by EGR1. Mechanistically, TENM3-AS1 reprograms FA metabolism, particularly enhancing FA biosynthesis, thereby promoting GC metastasis through direct interaction with hnRNPK and stabilizing hnRNPK-bound FASN mRNA. In summary, our research reveals that TENM3-AS1 is a promising biomarker and therapeutic target for abnormal FA reprogramming and GC metastasis.

Abbreviations

LncRNA	Long Non-Coding RNA
GC	Gastric Cancer
FA	Fatty Acid
TENM3-AS1	Teneurin Transmembrane Protein 3 Antisense 1
EGR1	Early Growth Response 1
hnRNPK	Heterogeneous Nuclear Ribonucleoprotein K
FASN	Fatty Acid Synthase
FISH	fluorescence in Situ Hybridization
RT-qPCR	Real-Time Quantitative PCR
ChIP	Chromatin Immunoprecipitation
RIP	RNA Immunoprecipitation
IHC	Immunohistochemical Analysis
HE	Hematoxylin-Eosin Staining Assay
CHX	Cycloheximide
OS	Overall Survival
PFS	Progression-Free Survival
DSS	Disease-Specific Survival
SYSUCC	Sun Yat-sen University Cancer Center
DAPI	4′,6-diamidino-2-phenylindole
TCGA	The Cancer Genome Atlas database
STAD	Stomach Adenocarcinoma
AJCC	American Joint Committee on Cancer
TSS	transcription start site
DEG	differentially expressed gene
GO	Gene Ontology database
KEGG	Kyoto Encyclopedia of Genes and Genomes database
KH	K homology domain
KI	K interactive domain
shRNA	Short hairpin RNA
siRNA	Small interfering RNA

Supplementary Information

The online version contains supplementary material available at https://doi.org/10.1186/s12943-025-02341-7.

Supplementary Material 1

Supplementary Material 2

Supplementary Material 3

Acknowledgements
We are grateful to the contributors to the public databases utilized in this study and the readers for their constructive and helpful comments.

Author contributions
YL, XZ, and WZ were responsible for the conception, design, and study supervision. YT, JZ, YX, YC, and FL collected clinical specimens and public data. WW provided the guidance for the experiments' methods. YT conducted experiments in the study. YT and BZ analyzed and interpreted data from the experiments. YT wrote the manuscript. YT, BZ, and HC revised the manuscript. All authors read and approved the final manuscript.

Funding
The work was supported by the Basic and Applied Basic Research Foundation of Guangdong Province (2022A1515012458, Yuanfang Li).

Data availability
No datasets were generated or analysed during the current study.

Declarations

Ethics approval and consent to participate
This study was approved by the Ethics Committee of Sun Yat-sen University Cancer Center (SZR2021-087), and informed consent was offered by each patient involved in this research. The Institutional Animal Care and Use Committee of SYSUCC approved all animal experiments in this study (Protocol L102022021003Q).

Consent for publication
All authors give consent for the publication of the manuscript.

Competing interests
The authors declare no competing interests.

Author details
[1]State Key Laboratory of Oncology in South China, Guangdong Provincial Clinical Research Center for Cancer, Sun Yat-sen University Cancer Center, Guangzhou 510060, P. R. China
[2]The Sixth Affiliated Hospital, South China University of Technology, Foshan 528000, P. R. China
[3]Zhongshan School of Medicine, Sun Yat-sen University, Guangzhou 510080, P. R. China
[4]Department of Medical Oncology, Guangdong Provincial Key Laboratory of Colorectal and Pelvic Floor Diseases, The Sixth Affiliated Hospital of Sun Yat-Sen University, Guangzhou 510655, P. R. China

Received: 4 December 2024 / Accepted: 22 April 2025
Published online: 06 June 2025

References

1. Bray F, Laversanne M, Sung H, Ferlay J, Siegel RL, Soerjomataram I, et al. Global cancer statistics 2022: GLOBOCAN estimates of incidence and mortality worldwide for 36 cancers in 185 countries. CA Cancer J Clin. 2024;74(3):229–63.
2. Lei ZN, Teng QX, Tian Q, Chen W, Xie Y, Wu K, et al. Signaling pathways and therapeutic interventions in gastric cancer. Signal Transduct Target Ther. 2022;7(1):358.
3. Ma S, Zhou M, Xu Y, Gu X, Zou M, Abudushalamu G, et al. Clinical application and detection techniques of liquid biopsy in gastric cancer. Mol Cancer. 2023;22(1):7.
4. Yao JC, Tseng JF, Worah S, Hess KR, Mansfield PF, Crane CH, et al. Clinicopathologic behavior of gastric adenocarcinoma in Hispanic patients: analysis of a single institution's experience over 15 years. J Clin Oncol. 2005;23(13):3094–103.
5. Cortes-Guiral D, Hubner M, Alyami M, Bhatt A, Ceelen W, Glehen O, et al. Primary and metastatic peritoneal surface malignancies. Nat Rev Dis Primers. 2021;7(1):91.
6. Hanahan D. Hallmarks of cancer: new dimensions. Cancer Discov. 2022;12(1):31–46.
7. Martinez-Reyes I, Chandel NS. Cancer metabolism: looking forward. Nat Rev Cancer. 2021;21(10):669–80.
8. Ye J, Wu S, Quan Q, Ye F, Zhang J, Song C, et al. Fibroblast growth factor receptor 4 promotes Triple-Negative breast Cancer progression via regulating fatty acid metabolism through the AKT/RYR2 signaling. Cancer Med. 2024;13(23):e70439.
9. Martin-Perez M, Urdiroz-Urricelqui U, Bigas C, Benitah SA. The role of lipids in cancer progression and metastasis. Cell Metab. 2022;34(11):1675–99.
10. Won Y, Jang B, Lee SH, Reyzer ML, Presentation KS, Kim H, et al. Oncogenic fatty acid metabolism rewires energy supply chain in gastric carcinogenesis. Gastroenterology. 2024;166(5):772–86. e14.
11. Castagnoli L, Corso S, Franceschini A, Raimondi A, Bellomo SE, Dugo M, et al. Fatty acid synthase as a new therapeutic target for HER2-positive gastric cancer. Cell Oncol (Dordr). 2023;46(3):661–76.
12. Pan J, Fan Z, Wang Z, Dai Q, Xiang Z, Yuan F, et al. CD36 mediates palmitate acid-induced metastasis of gastric cancer via AKT/GSK-3beta/beta-catenin pathway. J Exp Clin Cancer Res. 2019;38(1):52.
13. Yi Q, Feng J, Lan W, Shi H, Sun W, Sun W. CircRNA and lncRNA-encoded peptide in diseases, an update review. Mol Cancer. 2024;23(1):214.
14. Liu Y, Liu Y, Ye S, Feng H, Ma L. A new ferroptosis-related signature model including messenger RNAs and long non-coding RNAs predicts the prognosis of gastric cancer patients. J Transl Int Med. 2023;11(2):145–55.
15. Yuan Y, Han X, Zhao X, Zhang H, Vinograd A, Bi X, et al. Circulating exosome long non-coding RNAs are associated with atrial structural remodeling by increasing systemic inflammation in atrial fibrillation patients. J Transl Int Med. 2024;12(1):106–18.
16. Liu C, Shen A, Song J, Cheng L, Zhang M, Wang Y, et al. LncRNA-CCAT5-mediated crosstalk between Wnt/beta-Catenin and STAT3 signaling suggests novel therapeutic approaches for metastatic gastric cancer with high Wnt activity. Cancer Commun (Lond). 2024;44(1):76–100.
17. Han J, Nie M, Chen C, Cheng X, Guo T, Huangfu L, et al. SDCBP-AS1 destabilizes beta-catenin by regulating ubiquitination and sumoylation of HnRNP K to suppress gastric tumorigenicity and metastasis. Cancer Commun (Lond). 2022;42(11):1141–61.
18. Jia Y, Yan Q, Zheng Y, Li L, Zhang B, Chang Z, et al. Long non-coding RNA NEAT1 mediated RPRD1B stability facilitates fatty acid metabolism and lymph node metastasis via c-Jun/c-Fos/SREBP1 axis in gastric cancer. J Exp Clin Cancer Res. 2022;41(1):287.
19. Wang Z, Yang L, Wu P, Li X, Tang Y, Ou X, et al. The circROBO1/KLF5/FUS feedback loop regulates the liver metastasis of breast cancer by inhibiting the selective autophagy of Afadin. Mol Cancer. 2022;21(1):29.
20. Tang Y, Tian W, Zheng S, Zou Y, Xie J, Zhang J et al. Dissection of FOXO1-Induced LYPLAL1-DT impeding Triple-Negative breast Cancer progression via mediating hnRNPK/beta-Catenin complex. Research (Wash D C). 2023;6:0289.
21. Zheng S, Yang L, Zou Y, Liang JY, Liu P, Gao G, et al. Long non-coding RNA HUMT hypomethylation promotes lymphangiogenesis and metastasis via activating FOXK1 transcription in triple-negative breast cancer. J Hematol Oncol. 2020;13(1):17.
22. Tian W, Zhu L, Luo Y, Tang Y, Tan Q, Zou Y, et al. Autophagy deficiency induced by SAT1 potentiates tumor progression in Triple-Negative breast Cancer. Adv Sci (Weinh). 2024;11(36):e2309903.
23. Ferrer J, Dimitrova N. Transcription regulation by long non-coding RNAs: mechanisms and disease relevance. Nat Rev Mol Cell Biol. 2024;25(5):396–415.
24. Nguyen PL, Ma J, Chavarro JE, Freedman ML, Lis R, Fedele G, et al. Fatty acid synthase polymorphisms, tumor expression, body mass index, prostate cancer risk, and survival. J Clin Oncol. 2010;28(25):3958–64.
25. Peng WZ, Liu JX, Li CF, Ma R, Jie JZ. HnRNPK promotes gastric tumorigenesis through regulating CD44E alternative splicing. Cancer Cell Int. 2019;19:335.
26. Siomi H, Matunis MJ, Michael WM, Dreyfuss G. The pre-mRNA binding K protein contains a novel evolutionarily conserved motif. Nucleic Acids Res. 1993;21(5):1193–8.
27. Nakamoto MY, Lammer NC, Batey RT, Wuttke DS. HnRNPK recognition of the B motif of Xist and other biological RNAs. Nucleic Acids Res. 2020;48(16):9320–35.

28. Tan YT, Lin JF, Li T, Li JJ, Xu RH, Ju HQ. LncRNA-mediated posttranslational modifications and reprogramming of energy metabolism in cancer. Cancer Commun (Lond). 2021;41(2):109–20.
29. Yang X, Wen Y, Liu S, Duan L, Liu T, Tong Z et al. LCDR regulates the integrity of lysosomal membrane by HnRNP K-stabilized LAPTM5 transcript and promotes cell survival. Proc Natl Acad Sci U S A. 2022;119(5).
30. Tian C, Abudoureyimu M, Lin X, Chu X, Wang R. Linc-ROR facilitates progression and angiogenesis of hepatocellular carcinoma by modulating DEPDC1 expression. Cell Death Dis. 2021;12(11):1047.
31. Xi Z, Huang H, Hu J, Yu Y, Ma X, Xu M, et al. LINC00571 drives Tricarboxylic acid cycle metabolism in triple-negative breast cancer through HNRNPK/ILF2/IDH2 axis. J Exp Clin Cancer Res. 2024;43(1):22.
32. Liu SJ, Dang HX, Lim DA, Feng FY, Maher CA. Long noncoding RNAs in cancer metastasis. Nat Rev Cancer. 2021;21(7):446–60.
33. Adams BD, Parsons C, Walker L, Zhang WC, Slack FJ. Targeting noncoding RNAs in disease. J Clin Invest. 2017;127(3):761–71.
34. Li XC, Wang MY, Yang M, Dai HJ, Zhang BF, Wang W, et al. A mutational signature associated with alcohol consumption and prognostically significantly mutated driver genes in esophageal squamous cell carcinoma. Ann Oncol. 2018;29(4):938–44.
35. Kim TK, Shiekhattar R. Architectural and functional commonalities between enhancers and promoters. Cell. 2015;162(5):948–59.
36. Liu HT, Liu S, Liu L, Ma RR, Gao P. EGR1-Mediated transcription of lncRNA-HNF1A-AS1 promotes Cell-Cycle progression in gastric Cancer. Cancer Res. 2018;78(20):5877–90.
37. Ma Z, Gao X, Shuai Y, Wu X, Yan Y, Xing X, et al. EGR1-mediated linc01503 promotes cell cycle progression and tumorigenesis in gastric cancer. Cell Prolif. 2021;54(1):e12922.
38. Shuai Y, Ma Z, Liu W, Yu T, Yan C, Jiang H, et al. TEAD4 modulated LncRNA MNX1-AS1 contributes to gastric cancer progression partly through suppressing BTG2 and activating BCL2. Mol Cancer. 2020;19(1):6.
39. Jin Y, Wang C, Zhang B, Sun Y, Ji J, Cai Q, et al. Blocking EGR1/TGF-beta1 and CD44s/STAT3 crosstalk inhibits peritoneal metastasis of gastric Cancer. Int J Biol Sci. 2024;20(4):1314–31.
40. Liu Y, Kimpara S, Hoang NM, Daenthanasanmak A, Li Y, Lu L, et al. EGR1-mediated metabolic reprogramming to oxidative phosphorylation contributes to ibrutinib resistance in B-cell lymphoma. Blood. 2023;142(22):1879–94.
41. Wang B, Wang Y, Wang W, Wang Z, Zhang Y, Pan X, et al. WTAP/IGF2BP3 mediated m6A modification of the EGR1/PTEN axis regulates the malignant phenotypes of endometrial cancer stem cells. J Exp Clin Cancer Res. 2024;43(1):204.
42. Zheng L, Pu J, Jiang G, Weng M, He J, Mei H, et al. Abnormal expression of early growth response 1 in gastric cancer: association with tumor invasion, metastasis and heparanase transcription. Pathol Int. 2010;60(4):268–77.
43. Myung E, Park YL, Kim N, Chung CY, Park HB, Park HC, et al. Expression of early growth response-1 in human gastric cancer and its relationship with tumor cell behaviors and prognosis. Pathol Res Pract. 2013;209(11):692–9.
44. Tufail M, Jiang CH, Li N. Altered metabolism in cancer: insights into energy pathways and therapeutic targets. Mol Cancer. 2024;23(1):203.
45. Snaebjornsson MT, Janaki-Raman S, Schulze A. Greasing the wheels of the Cancer machine: the role of lipid metabolism in Cancer. Cell Metab. 2020;31(1):62–76.
46. Ferraro GB, Ali A, Luengo A, Kodack DP, Deik A, Abbott KL, et al. Fatty acid synthesis is required for breast Cancer brain metastasis. Nat Cancer. 2021;2(4):414–28.
47. Xu L, Zhang Y, Lin Z, Deng X, Ren X, Huang M, et al. FASN-mediated fatty acid biosynthesis remodels immune environment in Clonorchis sinensis infection-related intrahepatic cholangiocarcinoma. J Hepatol. 2024;81(2):265–77.
48. Wong TL, Loh JJ, Lu S, Yan HHN, Siu HC, Xi R, et al. ADAR1-mediated RNA editing of SCD1 drives drug resistance and self-renewal in gastric cancer. Nat Commun. 2023;14(1):2861.
49. Liu HH, Xu Y, Li CJ, Hsu SJ, Lin XH, Zhang R, et al. An SCD1-dependent mechanoresponsive pathway promotes HCC invasion and metastasis through lipid metabolic reprogramming. Mol Ther. 2022;30(7):2554–67.
50. Jiang T, Qi J, Xue Z, Liu B, Liu J, Hu Q, et al. The m(6)A modification mediated-lncRNA POU6F2-AS1 reprograms fatty acid metabolism and facilitates the growth of colorectal cancer via upregulation of FASN. Mol Cancer. 2024;23(1):55.
51. Liu S, Sun Y, Hou Y, Yang L, Wan X, Qin Y, et al. A novel LncRNA ROPM-mediated lipid metabolism governs breast cancer stem cell properties. J Hematol Oncol. 2021;14(1):178.
52. He Q, Yang C, Xiang Z, Huang G, Wu H, Chen T, et al. LINC00924-induced fatty acid metabolic reprogramming facilitates gastric cancer peritoneal metastasis via hnRNPC-regulated alternative splicing of Mnk2. Cell Death Dis. 2022;13(11):987.
53. Qin G, Tu X, Li H, Cao P, Chen X, Song J, et al. Long noncoding RNA p53-Stabilizing and activating RNA promotes p53 signaling by inhibiting heterogeneous nuclear ribonucleoprotein K desumoylation and suppresses hepatocellular carcinoma. Hepatology. 2020;71(1):112–29.
54. Li D, Wang X, Mei H, Fang E, Ye L, Song H, et al. Long noncoding RNA pancEts-1 promotes neuroblastoma progression through hnRNPK-Mediated beta-Catenin stabilization. Cancer Res. 2018;78(5):1169–83.

Publisher's note